Available online at www.sciencedirect.com
ScienceDirect
Biochimica et Biophysica Acta 1770 (2007) 1620–1626
Biochimica et Biophysica Acta BBA
www.elsevier.com/locate/bbagen

# Using giant unilamellar lipid vesicle micro-patterns as ultrasmall reaction containers to observe reversible ATP synthesis/hydrolysis of $F_0F_1$-ATPase directly

Xiaolong Liu [a,b], Rui Zhao [c], Yun Zhang [b], Xingyu Jiang [c], Jiachang Yue [b,*], Peidong Jiang [a], Zhenxi Zhang [a]

[a] *The Key Laboratory of Biomedical Information Engineering of Education Ministry, School of Life Science and Technology, Xi'an Jiaotong University, Xi'an 710049, China*
[b] *The National Laboratory of Biomacromolecules, Institute of Biophysics, Chinese Academy of Sciences, Beijing 100101, China*
[c] *National Centre for Nanoscience and Technology, Beijing 100103, China*

Received 10 May 2007; received in revised form 1 August 2007; accepted 1 August 2007
Available online 19 August 2007

**Abstract**

$F_0F_1$-ATPase within chromatophores, which was labeled with pH-sensitive quantum dots, was encapsulated in large unilamellar lipid vesicles (LUVs) through reverse-phase evaporation. Then a microarray of chromatophore-containing LUVs was created using a micro-contact printing (μ-CP) technique. Through controlled dehydration–rehydration of the lipid patterns, a microarray of single chromatophore-containing giant unilamellar lipid vesicles (GUVs) was formed with desired size and uniform shape. The reversible ATP synthesis/hydrolysis of $F_0F_1$-ATPase in GUVs was directly observed by fluorescence microscopy through the fluorescence intensity increase/decrease in the pH-sensitive quantum dots labeled on the outer surface of the chromatophore. To the best of our knowledge, this is the first direct observation of the reversible behavior of $F_0F_1$-ATPase at the bulk scale.


*Keywords:* $F_0F_1$-ATPase; Micro-contact printing (μ-CP); Giant unilamellar lipid vesicle (GUVs); Quantum dots; Chromatophore

Biochemical reactions always occur with very few reactants in confined spaces ranging from several nanometers to several micrometers. As well as the notion that confined chemistry will play an important role in nanotechnology, it is anticipated that reaction in a microenvironment approximating a biological system will reveal the nature of biological reactions *in vivo*. Therefore, improving experimental techniques to investigate and evaluate compartmentalized reactions under controlled conditions will become more and more important. As ultrasmall reaction containers, lipid vesicles are ideally suited to these kinds of investigations. Giant unilamellar vesicles (GUVs) are cell-sized liposomes composed of a single lipid bilayer with an entrapped aqueous compartment. They can hold extremely small volumes of liquid in their interior, giving researchers a unique insight and understanding into how biochemical reactions occur. It has been reported that they can be used to mimic natural biological environments for studies of biochemical reaction dynamics [1–3], single-molecule behavior [4], synchronized population behavior of enzymes in confined spaces [5], diffusible behavior of biological molecules [3,6], enzyme-catalyzed reactions [7,8], exocytosis [9], nanofluidic networks [10,11], bioanalytical applications and biosensors [12]. In biological systems such as single cells, the parallel handling of small numbers of molecules is inherent. A surfactant membrane, which plays a key role in biological molecule transportation, packaging, and sorting, provides the only workable biological reaction environment for a single or a few molecules. GUVs that have features of confined space and that mimic the cellular membrane would be very suitable for researching confined biological reactions *in vitro*.

*Abbreviations:* μ-CP, micro-contact printing; LUVs, large unilamellar lipid vesicles; GUVs, giant unilamellar lipid vesicle; SEM, scanning electron microscope; PDMS, polydimethylsiloxane; PMF, proton-motive force; CdTe, cadmium telluride

* Corresponding author.
*E-mail address:* yuejc@sun5.ibp.ac.cn (J. Yue).

0304-4165/$ - see front matter © 2007 Elsevier B.V. All rights reserved.
doi:10.1016/j.bbagen.2007.08.001

Micro-contact printing (μ-CP) is a widely used technique for patterning of biomolecules on a desired surface, such as protein, DNA/RNA, lipids [13,14]. Patterning of supported lipid bilayer microarrays has been demonstrated with various methods [14], however, producing GUV microarrays with desirable diameters and shapes has not yet been reported.

$F_0F_1$-ATPase is composed of two functional linked parts — $F_0$ and $F_1$. This complex catalyzes endergonic synthesis of ATP from ADP and phosphate using a transmembrane proton-motive force (PMF) generated by oxidative phosphorylation or photosynthesis [15–17]. In *Escherichia coli,* $F_0$ and $F_1$ are composed of $ab_2c_n$ and $\alpha_3\beta_3\gamma\delta\varepsilon$, respectively. These two parts are structurally linked by two stalks, a central stalk of γ and ε subunits which links to the c subunit ring and an outer stalk of $\delta b_2$, linking $\alpha_3$ to a subunit. The downhill proton flux through $F_0$ drives rotation of the c-ring and hence γ and ε, forcing a conformational change in $F_1$ that results in ATP synthesis from ADP and Pi. Conversely, ATP hydrolysis in $F_1$ causes reverse rotation of the rotor that drives $F_0$ to pump protons in the reverse direction. The exact mechanism of the reversible cycle of $F_0F_1$-ATPase is well known [18]. The reversible ATP synthesis/hydrolysis of $F_1$ and reversible proton flux through $F_0$ in intact $F_0F_1$-ATPase driven by an external mechanical force have been demonstrated at the single molecular level [19,20]. However, direct observation of the automatic reversible ATP synthesis/hydrolysis of natural $F_0F_1$-ATPase at the bulk scale has not yet been reported.

In this paper, we further developed the μ-CP technique to form chromatophore-containing GUV microarrays through controlled dehydration–rehydration, and directly observed reversible ATP synthesis/hydrolysis of $F_0F_1$-ATPase which was indicated by the fluorescence intensity change of pH-sensitive quantum dots labeled on the outer surface of chromatophores, in GUV patterns with different feature sizes. The schematic view of our experimental set-up is shown in Fig. 1.

## 1. Materials and methods

### 1.1. Chemical and materials

Esco microscope cover glass and ADP were purchased from Sigma-Aldrich CO. (St. Louis, USA). All other analytically purified reagents were purchased domestically.

Tricine–NaOH buffer (0.1 mM Tricine, 5 mM $MgCl_2$, 5 mM KCl, pH8). ATP synthesis buffer (50 mM Tris–HCl, 5 mM $MgCl_2$, 5 mM $K_2HPO_4$, 10% glycerol, pH 8.5). PBS buffer (137 mm NaCl, 2.7 mm KCl, 1.4 mm $KH_2PO_4$, 25 mm $Na_2HPO_4$, pH 7.4, 1% glycerol). Tris–HCl buffer (50 mM Tris–HCl, pH 6.5, 50 mM KCl, 2 mM $MgCl_2$). pH-sensitive quantum dots were synthesized by Prof. F.Q. Tang's group (Technical Institute of Physics and Chemistry, CAS).

Chromatophores were prepared from the cells of *Rhodospirillum rubrum* according to Ref [21,22].

### 1.2. Methods

#### 1.2.1. Synthesis of water-soluble pH-sensitive CdTe quantum dots

pH-sensitive quantum dots were synthesized by Prof. F.Q. Tang's group (Technical Institute of Physics and Chemistry, CAS) according to Ref [23]. In brief, the quantum dots were synthesized by adding freshly prepared NaHTe solution to nitrogen-saturated Cd(NO3)2 solutions at pH 8.5 in the presence of thiolglycolic acid (TGA) as a stabilizing agent. A small amount of ammonia was added in the solution as an additional stabilizing agent and pH controller because this would enable us to obtain high-quality quantum dots with a smaller size and a higher quantum yield. A series of quantum dots with sizes ranging from 2 to 5 nm were obtained, and in this work we used quantum dots with a maximum emission wavelength of 585 nm.

#### 1.2.2. Preparation of the micro-patterned polydimethylsiloxane (PDMS) stamps

A micro-patterned PDMS stamp was used for direct μ-CP as schematically shown in Fig. 1. The PDMS stamp was conventionally fabricated by a standard photolithographic technique [24]. In brief, a thin photoresist layer (15 μm, Shipley S1813) was spin-coated onto a silicon wafer and patterned photolithographically to produce a master. To imprint the patterns, PDMS monomers were poured on the photoresist and carefully peeled off after 4 h of curing at 100 °C. After its release, the PDMS stamp was sonicated in ethanol overnight to remove any residual siloxane monomers which could contaminate the glass, then the PDMS stamp served as the vehicle to transfer the ''ink''.

#### 1.2.3. Preparation of quantum dot labeled chromatophores

100 μL pH-sensitive quantum dots were added into 400 μL of chromatophores in Tris–HCl buffer (pH 6.5) at room temperature for 2 h, then the free fraction of quantum dots was washed three times by centrifugation (15000 rpm, 4 °C, 30 min). The precipitates were resuspended in 0.1 mM Tricine–NaOH buffer and stored at 4 °C before use.

#### 1.2.4. Preparation of chromatophore-containing large unilamellar vesicles

The chromatophore-containing LUVs were prepared by the standard reverse-phase evaporation method with some simplifications [25,26]. In brief, soybean lecithin was dissolved in chloroform with a final lipid concentration of 5 mg/mL. Then, 300 μL of lipid solution was transferred to a round-bottomed flask and the solvent was removed by rotary evaporation for 1 h at room temperature. A thin completely dry lipid film formed on the wall of the flask. Then, 4.5 mL of ether, 1.1 mL of ATP synthesis buffer, 200 μL of chromatophores, and 150 μL of methanol were carefully added into the flask, and protected by $N_2$. This mixture was sonicated in an ice-water bath for 20 min with a bath-type sonicator until a stable emulsion had completely formed. The organic solvent in the mixture was completely removed under reduced pressure with a rotary evaporator for 1 h at room temperature.

The chromatophore-containing LUVs were stored at 4 °C before use.

#### 1.2.5. Preparation of chromatophore-containing GUV patterns by controlled dehydration–rehydration

The micro-patterned PDMS stamp was used for direct micro-contact printing on a microscope cover glass. The cover glasses were cleaned with a mixture of $H_2SO_4$ and $H_2O_2$ (1:1) for 1 h, then thoroughly rinsed with DI-water and ethanol and dried in $N_2$ before use.

The stamp was covered with chromatophore-containing LUVs and subsequently dried in $N_2$. Then the stamp was placed on the cover glass for about 5 min without any external force and the chromatophore-containing LUVs were successfully transferred onto the cover glass. After the stamp had been removed, the substrate on which the pattern of LUVs had formed was dehydrated overnight in a vacuum drying oven under the protection of $N_2$. The chromatophore-containing GUVs were eventually formed by controlled rehydration of the dried LUV pattern in saturated water vapor.

ADP was injected into the chromatophore-containing GUVs through microinjection using a patch [12] to initiate ATP synthesis/hydrolysis at 37 °C. The fluorescence intensity of GUVs was observed with an Olympus IX71 fluorescence microscope and recorded by cooled digital CCD cameras (Princeton Scientific) with excitation at 515 nm and emission at 585 nm. The recorded images were processed with Winview/32 software (Princeton Scientific).

## 2. Results and discussion

### 2.1. Formation of regular chromatophore-containing GUV microarrays

We adopted the PDMS stamp with 4 μm features as template to create the LUV patterns, in which pH-sensitive quantum dot-

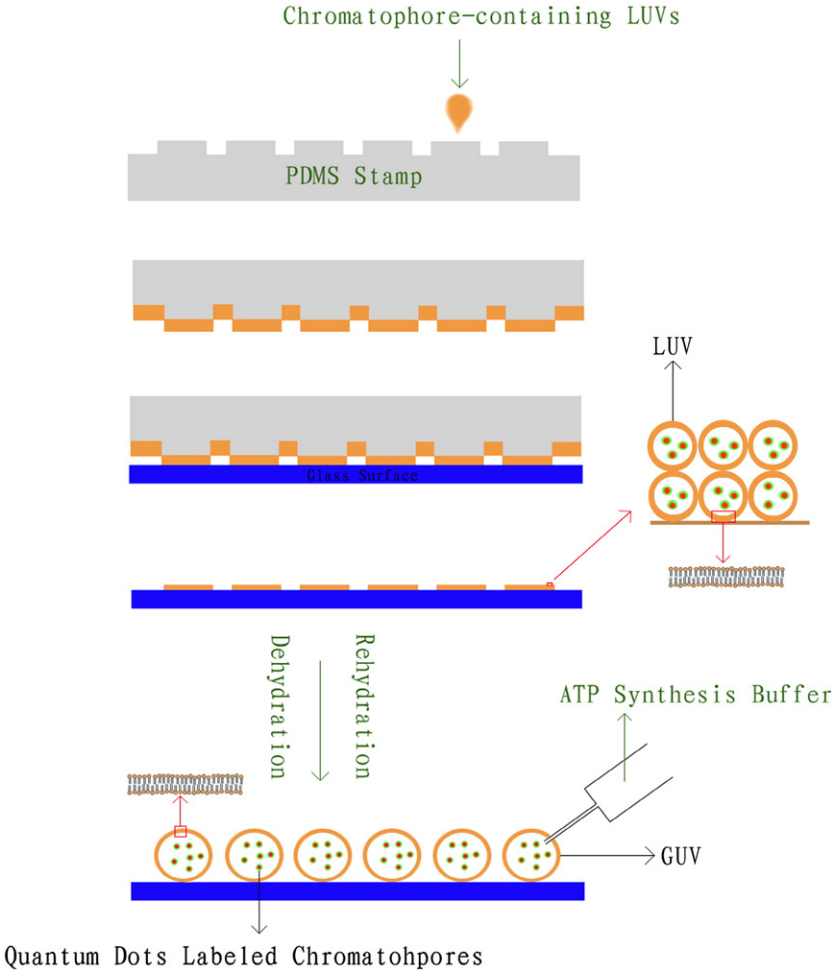


Fig. 1. Schematic view of micro-contact printing (μ-CP) of LUVs and the formation of GUVs.

labeled chromatophores were pre-encapsulated through the reverse phase evaporation technique. A scanning electron microscope (SEM) photo of the PDMS stamp is shown in Fig. 1 of Supporting material. Effective transfer of chromatophore-containing LUVs onto the cover glass surface was achieved. The single GUV patterns, which contained quantum dot-labeled chromatophores in the trapped aqueous space, were eventually formed by membrane fusion of LUVs when the cover glass was transferred to a saturated vapor environment. Fig. 2A shows a brightfield image of GUV patterns with 4 μm features. To confirm that the quantum dot-labeled chromatophores were encapsulated in the GUV patterns through the membrane fusion process, Fig. 2B shows a fluorescence image of GUV microarrays. The fluorescence intensity of the GUV pattern was not quenched by $CuCl_2$ (data not shown). This further demonstrated that the quantum dot-labeled chromatophores were not adsorbed on the outer surface of the GUVs. These GUVs formed by such a controlled dehydration–rehydration method have nearly uniform shape and size which were the same as the PDMS stamp (visible light image and fluorescence images of 50 μm GUV patterns are not shown). Fluorescence solution was also injected into the GUVs through a patch approach to demonstrate that the inclusion was not due to leakage (data not shown).

In our experimental process, these GUV microarrays could stabilize a few hours at room temperature or 37 °C in a saturated vapor environment (data not shown) [9,11,26], and all of our experiments were done in following 1 h after GUV generation.

Dehydration–rehydration is a widely used technique for producing GUVs [27,12]. In our work, the chromatophore-containing GUVs can also form by rehydration in PBS buffer with

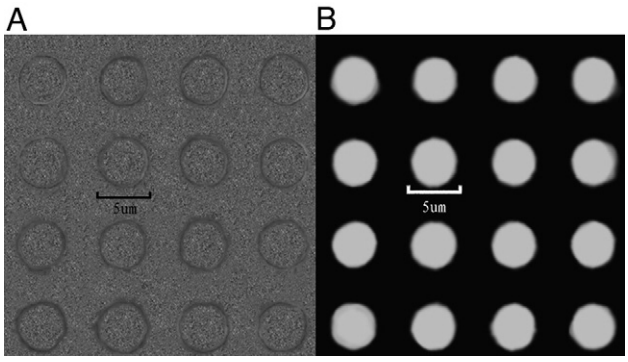


Fig. 2. (A) Chromatophore-containing GUV patterns formed by controlled dehydration–rehydration with 4-μm feature in diameter. (B) Fluorescence image corresponding to panel A.

size distribution from several micrometers to nearly 100 μm, but the pattern feature was entirely destroyed under such drastic hydration conditions (data were not shown). In contrast to drastic hydration conditions, the protocol described here adopted more gentle conditions in the rehydration process; under such gentle conditions, the energy of hydration is sufficient to fuse the LUVs to GUVs, but not enough to break the pattern feature. In this way, the pattern feature and desired size of GUVs can be achieved and controlled.

GUV patterns described here will be very attractive for use as ultrasmall reaction container microarrays, in which the reaction under study is confined and separated from the external medium. When each GUV is loaded with different reactants using injection methods, it could mimic a natural intracellular or intraorganellar environment with high throughput, which would be very useful in a variety of fields such as biodetection or the study of biochemical reaction dynamics.

### *2.2. Direct observation of reversible ATP synthesis/hydrolysis of $F_0F_1$-ATPase in GUV microarrays*

Here, we continued to use such GUV patterns to study the reversible ATP synthesis/hydrolysis of $F_0F_1$-ATPase within chromatophores. It is well known that $F_0F_1$-ATPase is a reversible ATP synthesis/hydrolysis molecular machine combined with reversible proton pump out/in. When the $F_1$-ATPase rotates clockwise, ATP is synthesized from ADP and phosphorus, and the protons are pumped out of the chromatophore. This causes a decrease in the pH value in the external environment. Conversely, hydrolysis of ATP results in counterclockwise rotation of $F_1$-ATPase and drives the pumping of protons into the chromatophore from the external environment. This causes an increase in pH value outside the chromatophores. Here, pH-sensitive quantum dots, which have a pH sensitivity range from 6 to 9, bound to the outer surface of the chromatophores through electrostatic force, then were used as the indicator for ATP synthesis/hydrolysis (shown in Fig. 2 of Supporting materials); the binding efficiency and detailed mechanism have already been published by our group [23]. The fluorescence intensity of quantum dots increases with the decrease in pH value in the external environment. So, these pH-sensitive quantum dots will be a reliable proton flux/efflux indicator in these ultrasmall reaction containers with confined volumes. The increase in fluorescence intensity in the GUVs reflects ATP synthesis, and the decrease in fluorescence intensity reflects ATP hydrolysis.

Fig. 3A shows a brightfield image of a GUV with 50 μm diameter (approximately 65 pL in volume) formed by rehydration in PBS buffer. ADP synthesis buffer with a final ADP concentration of 2 mM was injected with the patch approach to initiate the reversible ATP synthesis/hydrolysis reaction of $F_0F_1$-ATPase. Fig. 3B shows the time-lapse fluorescence image of GUV corresponding to Fig. 3A. In Fig. 3B, there are some

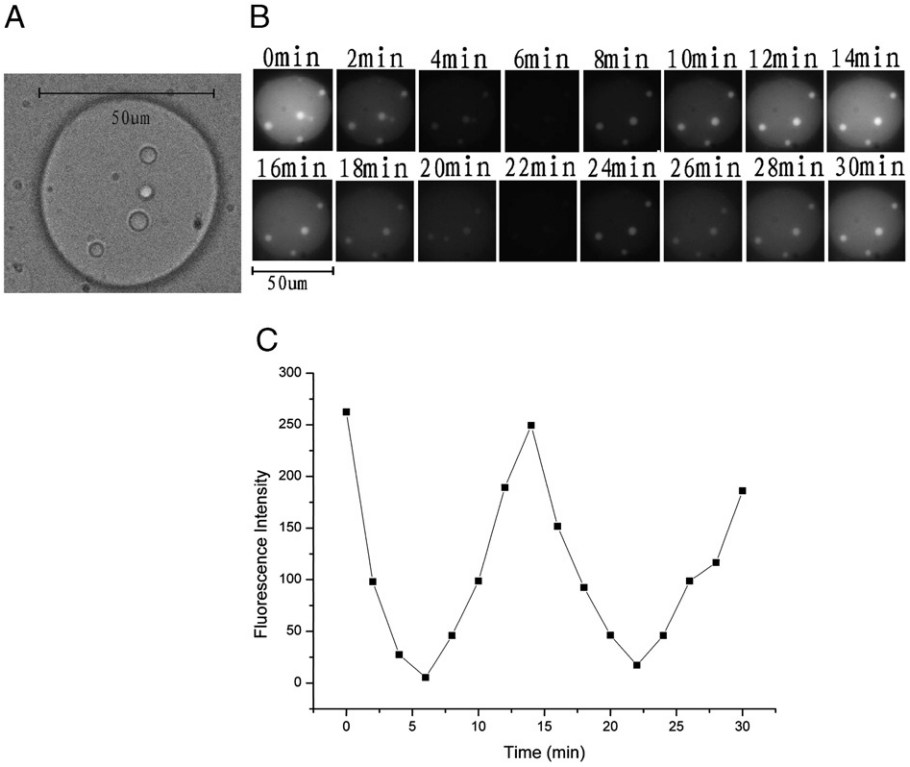


Fig. 3. (A) The visible light image of GUV with 50-μm feature which was formed by rehydration in PBS buffer; (B) reversible fluorescence intensity change of GUVs with 50-μm feature caused by reversible ATP synthesis/hydrolysis indicated by pH-sensitive quantum dots which were labeled on the outer surface of chromatophores. The small brighter circles inside the GUV are the assembled quantum dots labeled chromatophores; the fluorescence in the GUVs around the brighter circles is the dispersed quantum dots labeled chromatophores. (C) The fluorescence intensity curve corresponding to panel B.

brighter small circles inside the GUV; they are much more bigger than chomatophores (diameter around 60 nm in average), so they could be assembled quantum dot-labeled chromatophores. Fig. 3C shows the fluorescence intensity curve corresponding to Fig. 3B. According to Fig. 3B, it is clear that reversible ATP synthesis/hydrolysis can successfully initiate in such GUVs, but the microarray features of these GUVs were entirely destroyed by such drastic hydration conditions (data not shown).

Fig. 4A shows the time-lapse fluorescence images of GUV microarrays with 4 μm diameter feature size (approximately 32 fL in volume) undergoing reversible ATP synthesis/hydrolysis, while Fig. 4B shows the fluorescence intensity curve corresponding to Fig. 4A. These figures further confirm the previous results that these reactions can take place in much smaller spaces and under much gentler hydration conditions. These gentle conditions can retain the microarray feature of GUVs.

It can be seen from Figs. 3 and 4 that the reversible proton efflux/flux during ATP synthesis/hydrolysis can be detected sensitively. This was mainly because of the ultra-small volume of the GUV container and the ultra-sensitivity response of the quantum dots to pH change. When ADP is injected, the high ADP concentration will drive the $F_0F_1$-ATPase synthesis of ATP from ADP; when most of the ADP is consumed by $F_0F_1$-ATPase, there will be a higher ATP concentration than the ADP concentration in the solution. The higher ATP concentration will force $F_0F_1$-ATPase to change its conformation from synthesis status to hydrolysis status, and hydrolyze the synthesized ATP, then repeat the synthesis process. In this

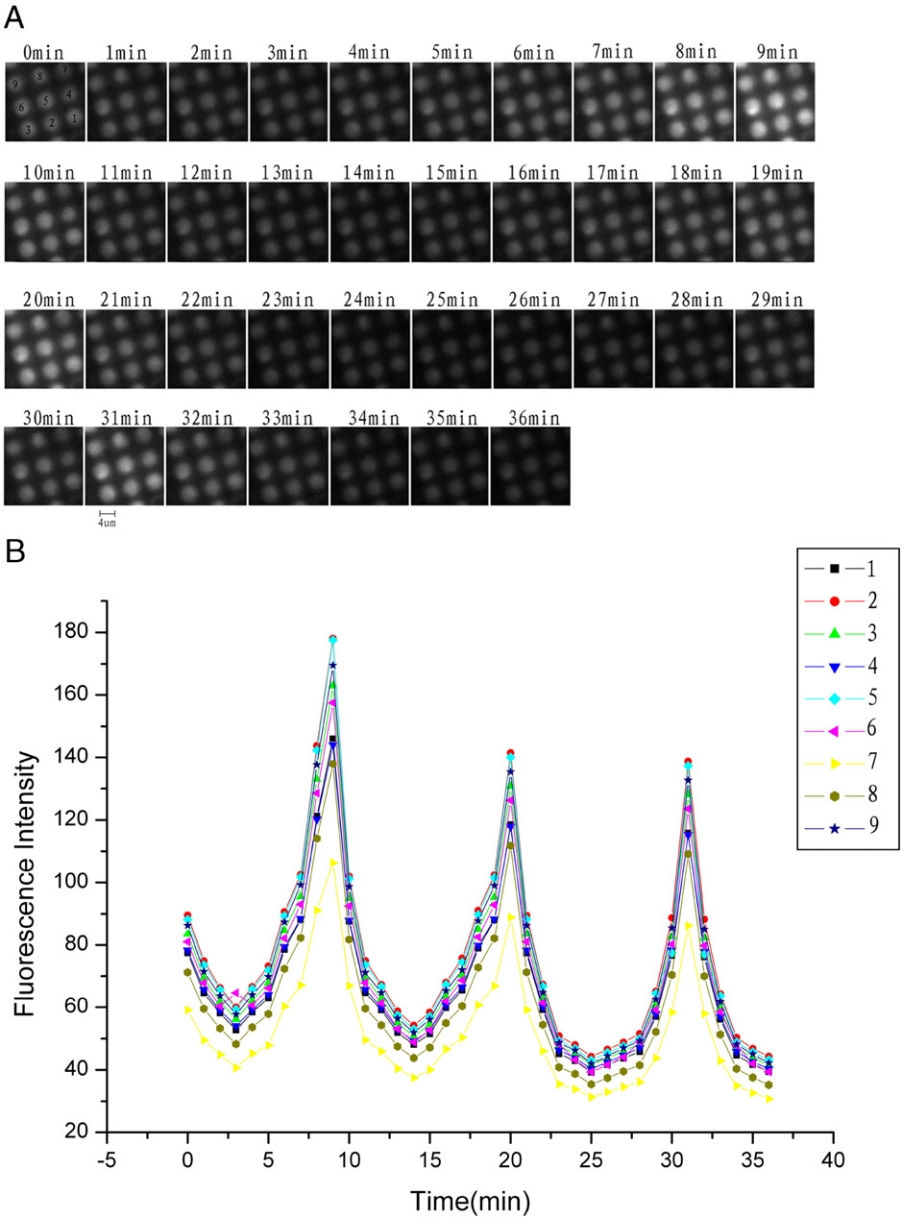


Fig. 4. (A) Reversible fluorescence intensity change of GUVs with 4-μm feature caused by reversible ATP synthesis/hydrolysis indicated by pH-sensitive quantum dots which were labeled on the outer surface of chromatophores; (B) the fluorescence intensity curves corresponding to panel A; 1, 2, 3 … 9 marked in panel A present the different GUVs, the corresponding intensity curve of the marked GUV was shown in panel B indicated by corresponding number.

way, a reversible cycle of ATP synthesis/hydrolysis can be produced. In this manner we believe that equilibrium between ATP and ADP concentrations will be reached, and then the reversible hydrolysis/synthesis cycle would stop, without further change in fluorescence intensity. In our experimental system, we did observe that most of the GUVs would stop working after several cycles (data not shown). But the detailed biochemical mechanism of the automatic reversible ATP synthesis hydrolysis/synthesis is still not clear and is being studied at the moment.

The cycle of reversible ATP synthesis/hydrolysis is about 5 min in such GUV patterns with a confined environment, and all of the GUV containers had very similar fluorescence oscillation frequencies. If all of the injected ADP (ATP) is consumed by $F_0F_1$-ATPase in each cycle, the ADP synthesis/hydrolysis velocity can be roughly estimated in such confined spaces. It was about 15.5ADP (ATP) $s^{-1}$ for each chromatophore ($F_0F_1$-ATPase) on average. This velocity is about 50% of the reported maximum rate of ATP synthesis/hydrolysis at room temperature [19].

The exact mechanism of reversible ATP synthesis/hydrolysis of $F_0F_1$-ATPase is well known, but such automatic reversible synthesis/hydrolysis in an artificial system has not been achieved before. Such automatic ATP/ADP oscillations in a biomimetic environment not only directly demonstrate the reversible mechanism of $F_0F_1$-ATPase, but also provide a potential application of such a device for energy storage.

## 3. Conclusion

In this work, we describe a method to generate controllable GUV patterns; then we used these GUV patterns to observe the reversible ATP hydrolysis/synthesis of $F_0F_1$-ATPase in a confined biomimetic environment directly. Automatic reversible fluorescence oscillation was achieved in such GUV patterns. To the best of our knowledge, this is the first time that the creation of GUV microarrays and the direct demonstration of the reversible ATP hydrolysis/synthesis behavior of $F_0F_1$-ATPase on a bulk scale have been reported.

The GUV patterns presented here also provide a tool that can be applied to study other confined biochemical reactions with high throughput, such as in developing biomimetic model systems for intracellular biochemical reactions, investigating a few or even single enzyme turnovers in a controlled environment, or serving as a platform for constructing complex biosensors.

Meanwhile, $F_0F_1$-ATPase will be an ideal motor and energy providing system for a micro/nanomachine because of its small size, smart and perfect structure, and ultra-high energy transfer efficiency [28]. Developing its automatic synthesis/hydrolysis will be very useful in micro/nanosystems for energy provision or energy storage for the extensively researched bio-motors such as kinesin or RNA motor. This can accelerate the engineering applications of such bio-motors. Furthermore, the periodically reversible fluorescence intensity oscillation of these GUV-patterns can also be used as a microarray in a low-frequency generator that would be very interesting for biomedical applications in the future.

## Acknowledgments

We thank Prof. Tang Fangqiong (Technical Institute of Physics and Chemistry, CAS) for kindly providing pH-sensitive quantum dots. This work was granted by programs of Natural Science Foundation of China (no: 30292905, 90306005, nanobiomedical and device application of CAS: Kjcx-sw-h12).

## Appendix A. Supplementary data

Supplementary data associated with this article can be found, in the online version, at doi:10.1016/j.bbagen.2007.08.001.

## References

[1] P. Bucher, A. Fisher, P.L. Luisi, T. Oberholzer, P. Walde, Giant vesicles as biochemical compartments: the use of microinjection techniques, Langmuir 14 (1998) 2712–2721.
[2] D.T. Chiu, C.F. Wilson, F. Ryttsén, A. Strömberg, C. Farre, A. Karlsson, S. Nordholm, A. Gaggar, B.P. Modi, A. Moscho, R.A. Garza-López, O. Orwar, R.N. Zare, Chemical transformations in individual ultrasmall biomimetic containers, Science 283 (1999) 1892–1895.
[3] T. Oberholzer, K.H. Nierhaus, P.L. Luisi, Protein expression in liposomes, Biochem. Biophys. Res. Commun. 261 (1999) 238–241.
[4] X.S. Xie, J.K. Trautman, Optical studies of single molecules at room temperature, Annu. Rev. Phys. Chem. 49 (1998) 441–480.
[5] P. Stange, D. Zanette, A. Mikhailov, B. Hess, Self-organizing molecular networks, Biophys. Chemist. 79 (1999) 233–247.
[6] D.T. Chiu, C. Wilson, A. Karlsson, A. Danielsson, A. Lundqvist, A. Strömberg, F. Ryttsén, M. Davidson, S. Nordholm, O. Orwar, R.N. Zare, Manipulating the biochemical nanoenvironment around single molecules contained within vesicles, Chem. Phys. 247 (1999) 133–139.
[7] H.P. Lu, L. Xun, X.S. Xie, Single-molecule enzymatic dynamics, Science 282 (1998) 1877–1882.
[8] A. Karlsson, K. Sott, M. Markstro1m, M. Davidson, Z. Konkoli, O. Orwar, Controlled initiation of enzymatic reactions in micrometer-sized biomimetic compartments, J. Phys. Chem., B 109 (2005) 1609–1617.
[9] A.S. Cans, N. Wittenberg, D. Eves, R. Karlsson, A. Karlsson, O. Orwar, A. Ewing, Amperometric detection of exocytosis in an artificial synapse, Anal. Chem. 75 (2003) 4168–4175.
[10] A. Karlsson, R. Karlsson, M. Karlsson, A.S. Cans, A. Strömberg, F. Ryttsén, O. Orwar, Networks of nanotubes and containers, Nature 409 (2001) 150–152.
[11] A. Karlsson, M. Karlsson, R. Karlsson, K. Sott, A. Lundqvist, M. Tokarz, O. Orwar, Nanofluidic networks based on surfactant membrane technology, Anal. Chem. 75 (2003) 2529–2537.
[12] M. Karlsson, K. Nolkrantz, M.J. Davidson, A. Strömberg, F. Ryttsén, B. Åkerman, O. Orwar, Electroinjection of colloid particles and biopolymers into single unilamellar liposomes and cells for bioanalytical applications, Anal. Chem. 72 (2000) 5857–5862.
[13] Y. Xia, J.A. Rogers, K. Paul, G.M. Whitesides, Unconventional methods for fabricating and patterning nanostructures, Chem. Rev. 99 (1999) 1823–1848.
[14] S.Y. Jung, M.A. Holden, P.S. Cremer, C.P. Collier, Two-component membrane lithography via lipid backfilling, Chem. Phys. Chem. 6 (2005) 423–426.
[15] P.D. Boyer, The ATP synthase — a splendid molecular machine, Annu. Rev. Biochem. 66 (1997) 717–749.
[16] J. Weber, A.E. Senior, ATP synthesis driven by proton transport in $F_1F_0$-ATP synthase, FEBS Lett. 545 (2003) 61–70.
[17] R.H. Fillingame, W. Jiang, O.Y. Dmitriev, P.C. Jones, Structural interpretations of $F_0$ rotary function in the *Escherichia coli* $F_1F_0$-ATP synthase, Biochim. Biophys. Acta 1458 (2000) 387–403.
[18] M. Yoshida, E. Muneyuki, T. Hisabori, ATP synthase — a marvellous rotary engine of the cell, Nat. Rev. Mol. Cell. Bio. 2 (2001) 669–677.

[19] H. Itoh, A. Takahashi, K. Adachi, H. Noji, R. Yasuda, M. Yoshida, K. Kinosita Jr., Mechanically driven ATP synthesis by $F_1$-ATPase, Nature 427 (2004) 465–468.
[20] X.L. Liu, X.A. Zhang, Y.B. Cui, J.C. Yue, Z.Y. Luo, P.D. Jiang, Mechanical driven proton conduction in single δ-free $F_0F_1$-ATPase, Biochem. Biophys. Res. Commun. 347 (2006) 752–757.
[21] G.E. Zippora, K. Daniel, Selective extraction and reconstitution of $F_1$ subunits from *Rhodospirillum rubrum* chromatophores, Methods Enzymol. 126 (1986) 528–538.
[22] S. Philosoph, A. Binder, G.E. Zippora, Coupling factor ATPase complex of *Rhodospirillum rubrum*, J. Biol. Chem. 252 (1977) 8747–8752.
[23] Y. Zhang, Z.T. Deng, J.C. Yue, F.Q. Tang, Q. Wei, Using cadmium telluride quantum dots as a proton flux sensor and applying to detect H9 avian influenza virus, Anal. Biochem. 364 (2007) 122–127.
[24] J.C. McDonald, G.M. Whitesides, Ploy(dimethylsiloxane) as a material for fabricating microfluidic devices, Accounts Chem. Res. 35 (2002) 491–499.
[25] F. Szoka Jr., D. Papahadjopoulos, Procedure for preparation of liposomes with large internal aqueous space and high capture by reverse-phase evaporation, Proc. Natl. Acad. Sci. U. S. A. 75 (1978) 4194–4198.
[26] W. Peter, I. Sosaku, Enzymes inside lipid vesicles: preparation, reactivity, and applications, Bioengineering 18 (2001) 143–177.
[27] M. Criado, B.U. Keller, A membrane fusion strategy for single-channel recordings of membranes usually non-accessible to patch-clamp pipette electrodes, FEBS Lett. 224 (1987) 172–176.
[28] T.M. Luo, R. Soong, E. Lan, B. Dunn, C. Montemagno, Photo-induced proton gradients and ATP biosynthesis produced by vesicles encapsulated in a silica matrix, Nat. Mater. 4 (2005) 220–224.